Joint Diseases and Related Surgery

Jt Dis Relat Surg
2026;37(x):i-xvi

ORIGINAL ARTICLE

The greater sciatic notch-based transcolumnar magic screw trajectory in the acetabulum: An anatomical guide

Pelin İsmailoğlu, PhD[1], Cengiz Kazdal, MD[2], Emrehan Uysal, MD[1], Alp Bayramoğlu, MD, PhD[3]

[1]Department of Anatomy, Recep Tayyip Erdoğan University Faculty of Medicine, Rize, Türkiye
[2]Student Recep Tayyip Erdoğan University Faculty of Medicine, Rize, Türkiye
[3]Department of Anatomy, Acıbadem Mehmet Ali Aydınlar University, İstanbul, Türkiye

ABSTRACT

Objectives: This study aims to define the greater sciatic notch (GSN)-based transcolumnar "magic screw" corridor in the acetabulum and to assess its morphometric characteristics and anatomical feasibility according to quadrilateral plate (QP) morphology.

Materials and methods: Between November 2025 and January 2026, three-dimensional morphometric analysis was performed on pelvic CT reconstructions of 90 adults (180 acetabulae) with intact pelvic bones and no evidence of hip or pelvic pathology. Using Mimics, pelvic models were reconstructed and a virtual 6.5-mm cannulated screw was advanced from the midpoint of the GSN toward the anterior column along a transcolumnar intraosseous trajectory. Bilateral trajectory length, angulation, and QP thickness were recorded. Differences by sex and side, age associations, and anatomical feasibility ("easy" versus "hard") were analyzed based on anatomical corridor constraints.

Results: Of the patients included in the study, 42 were male and 48 were female with a mean age of 49.88 ± 17.18 (range, 19 to 86) years. The defined GSN-based transcolumnar screw corridor was anatomically feasible in 94.44% of cases. Mean posterior acetabular screw length was 74.16 ± 7.49 mm right and 73.21 ± 6.90 mm left. Mean GSN entry segment length was 22.95 ± 4.14 mm right and 23.48 ± 4.34 mm left. Mean acetabular screw angles were 125.86 ± 6.05° right and 124.26 ± 5.24° left, with a small but significant right-left difference ($p = 0.004$). The QP morphology demonstrated substantial variability: mean maximum thickness was 14.87 ± 2.75 mm right and 14.77 ± 2.82 mm left, while minimum thickness was 3.46 ± 1.37 mm right and 3.48 ± 1.32 mm left. Men had significantly greater superior and posterior acetabular screw lengths and markedly thicker QP parameters compared with women (all $p \leq 0.027$), with large effect sizes for QP thickness ($d > 1.0$).

Conclusion: A GSN-based transcolumnar magic screw corridor appears anatomically feasible in most adult pelves and provides a quantifiable intraosseous trajectory reaching both acetabular columns. Quadrilateral plate thickness emerges as the main anatomical limiting factor, particularly in female pelves and in cases categorized as corridor-constrained.

Keywords: Acetabulum, computed tomography, magic screw, morphometry, posterior column, quadrilateral plate.

Pelvic and acetabular fractures account for a significant proportion of musculoskeletal injuries, representing around 3% to 8% of all fractures reported in trauma patients.[1] These injuries are associated with substantial morbidity and mortality, with reported in hospital mortality rates of 8.3% to 13.4%.[1,2] The primary goal of surgical management in such fractures is to achieve anatomical reduction by restoring the disrupted osseous alignment through accurate repositioning of fracture fragments.[3,4]

In complex acetabular fractures, particularly those involving multiple fracture lines, stabilization of both the anterior and posterior columns is often required to restore pelvic continuity and joint congruity.[5,6] The quadrilateral plate (QP), which forms the medial wall of the acetabulum, plays a key role in complex acetabular fracture patterns.[7-9] Quadrilateral plate involvement is observed in nearly 80% of acetabular fracture types,

Received: January 30, 2026
Accepted: April 17, 2026
Published online: July 13, 2026

Correspondence: Pelin İsmailoğlu, PhD. Recep Tayyip Erdoğan Üniversitesi Tıp Fakültesi, Anatomi Anabilim Dalı, 53020 Rize, Türkiye.

E-mail: pelin.ismailoglu@erdogan.edu.tr

Doi: 10.52312/jdrs.2026.2857

Citation: İsmailoğlu P, Kazdal C, Uysal E, Bayramoğlu A. The greater sciatic notch-based transcolumnar magic screw trajectory in the acetabulum: An anatomical guide. Jt Dis Relat Surg 2026;37(x):i-xvi. doi: 10.52312/jdrs.2026.2857.

including both-column, T-shaped and transverse fractures.[9] Managing the QP is challenging due to its deep anatomical location and thin cortical bone, which limits the options for traditional fixation.[10] Furthermore, the close proximity of the QP to the hip joint increases the risk of intra-articular screw penetration, while its medial location adjacent to pelvic viscera and neurovascular structures further complicates safe surgical access and implant placement.[5,9] Taken together, these anatomical constraints make stable fixation of the QP technically demanding and prone to complications, prompting the development of alternative fixation strategies.[7,10]

In this context, percutaneous screw techniques have gained increasing attention as minimally invasive options for achieving stable fixation of medial acetabular fractures while reducing soft-tissue disruption.[5,6] The so-called "magic screw" is a transcolumnar fixation technique designed to stabilize the QP through an antegrade intraosseous corridor.[9] Compared to conventional posterior column screw fixation, it may offer advantages such as easier positioning, less soft-tissue disruption and improved buttressing of the medial acetabular wall while maintaining a minimally invasive approach.[4] These potential advantages have driven increasing interest in anatomically guided percutaneous screw placement strategies for complex acetabular fracture patterns.[11-13] Importantly, the transcolumnar trajectory of the magic screw enables simultaneous stabilization of both acetabular columns through a single posterior entry point, potentially allowing fixation of complex fracture patterns without the need for intraoperative patient repositioning.[9]

Despite these theoretical and practical advantages, the magic screw technique has not yet gained widespread clinical adoption.[3,5,6] The principal limitation lies in the difficulty of defining a consistently safe and reproducible screw entry point and trajectory within the complex three-dimensional (3D) pelvic anatomy. Even minor deviations during screw insertion may result in cortical breach, intra-articular penetration, or injury to adjacent neurovascular structures.[1,9] In this regard, the thickness and morphological variability of the QP constitute critical anatomical factors influencing the safety of transcolumnar screw placement.[3]

Previous anatomical and technical studies have primarily focused on fluoroscopy-dependent strategies to facilitate magic screw placement.[14] Li et al.[9] established standardized fluoroscopic views and C-arm angulations that allow visualization of the screw corridor as a point projection, demonstrating that accurate placement is feasible when specific imaging conditions are met. However, reliance on precise intraoperative fluoroscopic positioning introduces practical limitations, including increased radiation exposure, variability related to patient positioning, and difficulty reproducing exact imaging angles in routine clinical settings.[9,14] In this context, identifying a consistent and surgically recognizable posterior anatomical landmark may help to address some of the practical limitations associated with fluoroscopy-dependent techniques. The greater sciatic notch (GSN) is a distinct osseous structure that can typically be visualized or palpated during posterior acetabular exposure and has been described as a potential reference point for guiding transacetabular screw trajectories.[15-17] Moreover, given its anatomical proximity to important neurovascular structures, careful trajectory planning based on regional anatomy may contribute to enhancing procedural safety.[16,18] Therefore, a standardized description of a transcolumnar screw corridor referenced to the GSN could potentially facilitate more consistent and clinically applicable fixation strategies. Although the GSN is a consistent posterior landmark, it has not been quantitatively defined as a standardized entry point for transcolumnar screw placement. [15-17]

In the present study, we aimed to establish an anatomy-based definition of a GSN-based transcolumnar magic screw corridor using 3D computed tomography (CT) reconstructions, to describe its morphometric characteristics, and to assess its feasibility with particular emphasis on QP morphology.

MATERIALS AND METHODS

This retrospective, observational, cross-sectional study was conducted at Recep Tayyip Erdoğan University Faculty of Medicine, Department of Anatomy between November 2025 and January 2026. Retrospective pelvic CT scans were retrieved from the radiology archive of Acıbadem Mehmet Ali Aydınlar University Altunizade Hospital. Scans were originally obtained for clinical reasons unrelated to an orthopedic evaluation, such as for assessing the gastrointestinal system, diagnosing urinary dysfunction, investigating abdominal pain. A total of 250 pelvic CT scans were initially screened. Only scans demonstrating intact acetabula with preserved cortical and trabecular bone morphology, and sufficient image quality for 3D reconstruction and morphometric analysis, were included. Review of pelvis CT examinations was conducted to ensure that the acquisition and reconstruction parameters were comparable and suitable for 3D morphometric analysis. The presence or absence of intravenous contrast administration was not considered, since all analyses were performed exclusively on bone-window CT datasets. Bone reconstructions were generated using standardized reconstruction parameters (including slice thickness, reconstruction kernel, and voxel size) to ensure methodological consistency. Scans were excluded if there was any history of, or imaging evidence for, pelvic trauma; acetabular or hip fractures; prior hip or pelvic surgery; degenerative hip disease (including advanced osteoarthritis); congenital pelvic or acetabular deformities; or pelvic or periacetabular malignancy. Scans with inadequate image quality or artefacts that precluded reliable 3D reconstruction were also excluded. Finally, a total of 90 pelvic CT scans were included in the final analysis. As both hips were evaluated separately for each patient, a total of 180 acetabulae were analyzed.

Eligible cases that fulfilled all the inclusion criteria and none of the exclusion criteria were selected consecutively from the archive to minimize selection bias. As the primary aim of the study was to characterize general anatomical feasibility parameters within an adult pelvic population, it was not necessary to apply any predefined demographic stratification during case selection. In line with institutional ethical regulations, all CT datasets were anonymized by the radiology department prior to transfer to the research team. Personal identifiers were removed, and DICOM files were reassigned with coded numerical IDs. The investigators had access only to demographic variables (age and sex) and imaging data. Given the retrospective design of the study and the use of fully anonymized institutional records, informed consent was obtained from all patients included in the study.

The study protocol was approved by the Acıbadem Mehmet Ali Aydınlar University Ethics Committee (ATADEK) (Date: 30.10.2025, No.: 2025-17/651). The study was conducted in accordance with the principles of the Declaration of Helsinki.

Computed tomography acquisition and three-dimensional reconstruction

All CT examinations were performed with the patient in the supine position using a multidetector CT system (Somatom Force; Siemens Healthineers, Erlangen, Germany). Imaging was conducted according to standard acquisition protocols, with the tube voltage set to 100 kVp and the tube current to 256 mAs. Axial images were obtained with a slice thickness ranging from 0.5 to 1.0 mm, reconstructed on a 512 × 512 matrix and exported with an approximate voxel size of 0.7 × 0.7 × 0.5 mm^3. The acquired datasets were reconstructed using a high-resolution bone algorithm and imported into Mimics® software (Materialise, Leuven, Belgium) for 3D processing. Patient-specific 3D pelvic models were generated from these datasets and served as the basis for all subsequent morphometric analyses and virtual screw placement simulations.

Definition of the transcolumnar magic screw trajectory

To anatomically simulate a posterior-entry magic screw that can engage both the posterior and anterior acetabular columns, a virtual screw model was created using commercially available 3D modelling software (Rhinoceros® 3D, McNeel, Seattle, WA, USA). The screw was designed to resemble a standard 6.5-mm cannulated acetabular screw, with sufficient length to traverse the acetabulum along a transcolumnar intraosseous path. The virtual screw model was, then, exported as a Standard Tessellation Language (STL) file and imported into Mimics® software. In each 3D pelvic model, the screw entry point was defined as the midpoint of the GSN. From this posterior entry point, the screw was advanced anteriorly through the posterior column toward the anterior column, following an intraosseous trajectory that remained entirely within the acetabular bone, avoiding both cortical breach and intra-articular penetration. For each case, the screw trajectory was iteratively adjusted to maximize intraosseous length while preserving a safe distance from the acetabular joint surface and the surrounding cortical boundaries. This optimized pathway is known as the GSN-based transcolumnar magic screw trajectory. Prior to taking morphometric measurements, digital pelvic realignment was performed in a 3D modelling environment. Standardized anatomical reference planes (sagittal, coronal, axial) were used to minimize variability related to pelvic rotation or positioning. The automatic orientation functions of the Mimics® software (anterior, posterior and lateral alignment commands) were also applied to ensure consistent positioning of all pelvic models. The final anatomical orientation of each pelvis was verified by two investigators involved in the study: an orthopedic surgeon and an anatomist.

Morphometric measurements

Morphometric analysis was performed using 3D pelvic models in Mimics® software. For each hemipelvis, the measurement process followed a standardized, stepwise protocol. All morphometric measurements were conducted by two independent blinded observers. Observer 1 (8 years of clinical experience in pelvic and acetabular trauma surgery) performed the first measurement series and repeated all measurements approximately six months later to assess intraobserver reliability. Observer 2 (10 years of experience in musculoskeletal morphology) independently performed the measurements in a blinded fashion to determine interobserver reliability.

Three consistent anatomical reference points were defined: (1) the midpoint of the GSN (GSN mid); (2) the superior acetabular rim (SAR); and (3) the posterior acetabular rim (PAR) (Figure 1). Based on these landmarks, trajectory-related linear (screw length) and angular parameters were measured, and the relative distances between the screw axis and each anatomical landmark were recorded (Figure 1). The midpoint of the GSN was defined geometrically on the 3D pelvic surface model as the linear midpoint between the superior and inferior cortical margins of the notch contour following standardized digital pelvic realignment. This landmark was identified under standardized software-aligned anatomical orientations and subsequently confirmed by systematic visual verification to ensure inter-case consistency. Trajectory optimization was performed manually using a standardized stepwise simulation protocol rather than an automated algorithm. Small predefined angular adjustments were applied under continuous multiplanar visualization to maximize intraosseous screw length while maintaining cortical containment and avoiding intra-articular penetration. During this optimization process, a consistent peripheral cortical safety margin of approximately 2 to 3 mm (corresponding to roughly half of the screw diameter) was preserved between the virtual screw surface and the outer cortical boundary (Figures 1-5). Trajectories approaching this predefined safety margin were considered unsafe and were readjusted accordingly.

The angle between the screw trajectory and the GSN reference was measured using the standardized lateral (BT) orientation view provided by the software. The angle between the screw trajectory and the SAR was measured using the posterior view automatically aligned by the software. Using this configuration, the effective screw entry length from the GSN was recorded (Figure 2).

From this reference point, a virtual 6.5 mm screw was advanced anteriorly along an intraosseous path toward the anterior pubic ramus. Trajectory containment and intra-articular safety were verified

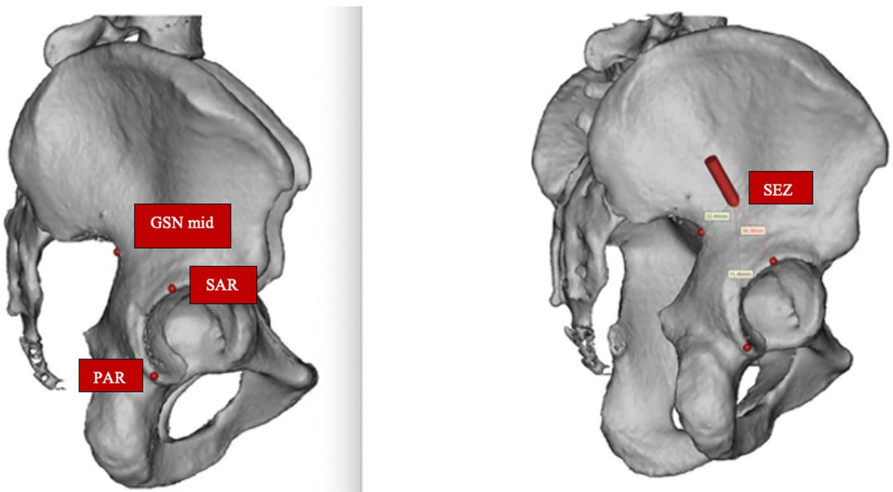

FIGURE 1. Anatomical reference landmarks used for morphometric analysis: Three-dimensional hemipelvic reconstruction illustrating the predefined anatomical reference points used for angular and linear measurements. The midpoint of the greater sciatic notch (GSN mid), the superior acetabular rim (SAR), and the posterior acetabular rim (PAR) were used as fixed anatomical landmarks for defining the transcolumnar trajectory. The screw entry zone (SEZ) indicates the posterior cortical penetration point corresponding to the virtual transcolumnar screw pathway.

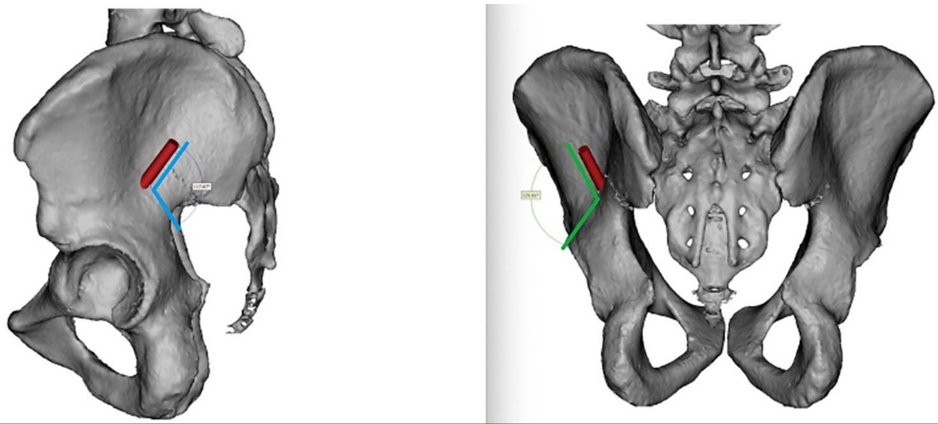

FIGURE 2. Angular assessment of the greater sciatic notch–based transcolumnar screw trajectory: Illustration of the virtual magic screw trajectory and the corresponding angular measurements obtained using standardized Mimics software-aligned views. The angle between the screw trajectory and the greater sciatic notch reference was measured in the lateral (CT) view, while the angle relative to the superior acetabular rim was assessed in the posterior view. These angles were used to characterize trajectory orientation and entry geometry.

in multiplanar views, including the coronal BT view (Figure 3).

Quadrilateral plate morphology was evaluated on a standardized cross-sectional plane defined by a line connecting the PAR and the anterior inferior iliac spine. In this section, the maximum and minimum thicknesses of the QP along the projected screw path were measured (Figure 4).

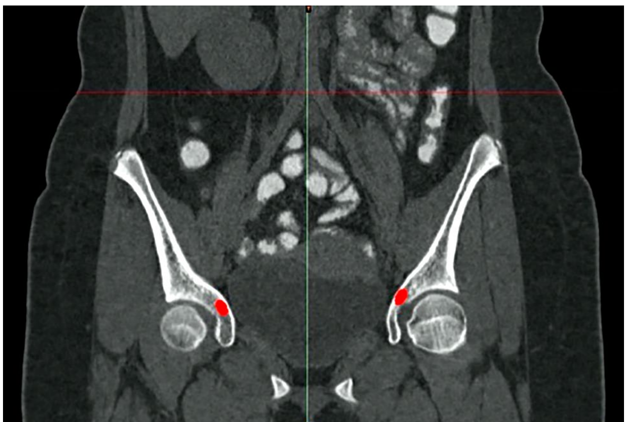

FIGURE 3. Coronal CT view demonstrating the posteroanterior orientation of the virtual 6.5-mm transcolumnar magic screw trajectory: The screw is inserted from the midpoint of the greater sciatic notch and advances anteriorly along an intraosseous pathway toward the anterior pubic ramus. The trajectory remains fully embedded within the osseous corridor without acetabular joint penetration. The red highlighted area represents the coronal projection of the screw pathway.

During virtual screw simulation, it was observed that a subset of pelves had a relatively smaller osseous morphology compared with the rest of the cohort. When the same GSN-based entry point and the standard trajectory objective were applied, specifically, aiming to embed the screw tip within the anterior pubic ramus as in the remaining pelves, the screw trajectory in these smaller pelves tended to violate the QP cortex, thereby resulting in extraosseous breach. To prevent QP perforation while maintaining the same posterior entry point, trajectory adjustments were attempted; however, in these cases the alternative trajectory that avoided thinner QP violation resulted in superior acetabular roof breach with intra-articular penetration (Figure 5). Accordingly, in pelves demonstrating this corridor constraint, a smaller-diameter screw model (5.5 mm) was used in place of the standard 6.5 mm screw to enable intraosseous placement while preserving cortical and articular safety. Pelves requiring this modification were recorded as anatomically "hard" for transcolumnar screw placement, whereas cases in which a 6.5 mm screw could be placed intraosseously without cortical breach or articular penetration were recorded as "easy." All morphometric measurements, including screw trajectory lengths, angular orientations and QP thickness parameters, were performed bilaterally for each pelvis and systematically recorded for analysis. All pelvic measurements were performed using the standardized, software-aligned anatomical views provided by Mimics. Specifically, the pelvis was

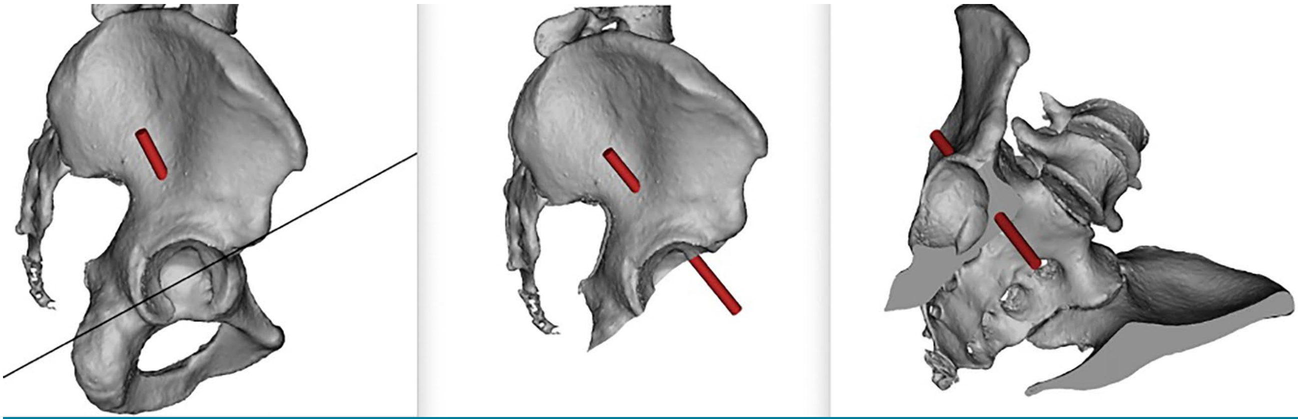

FIGURE 4. Assessment of quadrilateral plate morphology and anatomical feasibility: Cross-sectional plane defined by a line connecting the posterior acetabular rim and the anterior inferior iliac spine, illustrating measurement of maximum and minimum quadrilateral plate thickness along the projected screw path. This assessment was used to evaluate anatomical constraints influencing screw feasibility and to distinguish pelves classified as "easy" or "hard" for transcolumnar magic screw placement.

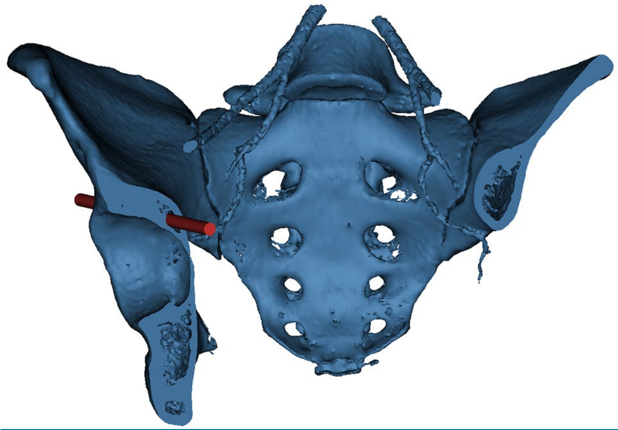

FIGURE 5. Illustration of the thin quadrilateral plate along the simulated transcolumnar screw corridor: Three-dimensional pelvic reconstruction showing the projected trajectory of the transcolumnar screw based on the greater sciatic notch and the corresponding region of reduced quadrilateral plate thickness. The image emphasizes the thin cortical wall at the screw exit region.

positioned in the Mimics automatic lateral (BT) orientation for lateral-plane measurements, and the remaining measurements were obtained according to the anterior/lateral/posterior auto-alignment to ensure consistency across cases.

Assessment of anatomical feasibility

Anatomical feasibility was classified as "easy" or "hard" based on whether a standard 6.5-mm intraosseous transcolumnar trajectory could be achieved without cortical breach or intra-articular violation. This feasibility classification was used solely for exploratory anatomical analysis and did not reflect intraoperative technical difficulty.

Statistical analysis

A post-hoc power analysis was performed using G*Power version 3.1 software (Heinrich Heine University Düsseldorf, Düsseldorf, Germany). Given that the largest and most consistent group differences were observed in QP thickness between female and male participants, Cohen's d values derived from these comparisons were used for power estimation. The lower bound of the observed large effect sizes ($d = 0.75$) was selected as a conservative estimate. With an alpha level of 0.05 (two-tailed) and the final group sizes (48 females and 42 males), the achieved statistical power ($1-\beta$) was calculated as 0.94. This indicates that the study was adequately powered to detect medium-to-large sex-related differences in acetabular and QP morphometry.

Statistical analysis was performed using the IBM SPSS version 26.0 software (IBM Corp., Armonk, NY, USA). Continuous variables were presented in mean ± standard deviation (SD) or median (min-max), while categorical variables were presented in number and frequency. Distributional assumptions were evaluated using skewness and kurtosis statistics. Following commonly accepted guidelines, absolute skewness values below 2 and absolute kurtosis values below 7 were considered indicative of approximate normality.[19-21] Given the moderate sample size and the robustness of parametric tests to modest deviations from normality, parametric analyses were considered appropriate. Comparisons between female and male participants were conducted using independent samples t-tests for all continuous morphometric parameters, and effect sizes were reported as Cohen's d. Side-to-side (right *vs.* left) differences were examined using paired samples t-tests, with Cohen's d reported for paired comparisons. Associations between age and morphometric parameters were evaluated using Pearson correlation analyses. For variables demonstrating statistically significant correlations with age, univariate linear regression models were subsequently performed to quantify the predictive effect of age on those outcomes; regression coefficients were reported. To explore whether morphometric parameters differed according to screw placement feasibility, cases categorized as "screw placement harder" versus "screw placement easier" were compared using independent-samples t-tests. Due to the markedly unbalanced group sizes, these analyses were treated as exploratory and interpreted cautiously. Inter- and intraobserver reliability were assessed using two-way mixed-effects intraclass correlation coefficients (ICC) with absolute-agreement and single-measure definitions. A two-tailed p value of < 0.05 was considered statistically significant.

RESULTS

Of the patients included in the study, 42 were male and 48 were female with a mean age of 49.88 ± 17.18 (range, 19 to 86) years. For the categorical variables related to screw placement difficulty, the majority of cases were classified as "screw placement easier." Screw placement was rated as "easier" in 85 cases (94.44%) and "harder" in five cases (5.56%). Descriptive statistics for screw lengths, screw angles, and QP thickness parameters are summarized in Table I. Skewness and kurtosis values indicated acceptable distributional characteristics.[20,21] Therefore, parametric tests were applied.

Overall, the dataset demonstrated balanced demographic features and consistent bilateral patterns across all first-measurement screw length, screw angle, and QP thickness parameters (Table I). Skewness and kurtosis values were within acceptable thresholds for assuming approximate

TABLE I
Descriptive statistics for demographic, morphometric, and procedural variables (n = 90)

	n	%	Mean ± SD	Skewness	Kurtosis
Age (year)			49.88 ± 17.18	0.00	–1.05
Right GSN screw length (mm)			22.95 ± 4.14	0.49	0.33
Left GSN screw length (mm)			23.48 ± 4.34	1.52	3.58
Right superior acetabular screw length (mm)			43.29 ± 6.71	0.42	–0.21
Left superior acetabular screw length (mm)			42.34 ± 6.54	0.49	0.42
Right posterior acetabular screw length (mm)			74.16 ± 7.49	0.27	–0.32
Left posterior acetabular screw length (mm)			73.21 ± 6.90	0.65	0.77
Right GSN screw angle (°)			111.91 ± 8.66	0.16	–0.28
Left GSN screw angle (°)			110.11 ± 8.98	-0.83	3.60
Right acetabular screw angle (°)			125.86 ± 6.05	0.16	0.26
Left acetabular screw angle (°)			124.26 ± 5.24	-0.18	–0.83
Right quadrilateral plate max thickness (mm)			14.87 ± 2.75	0.41	–0.32
Left quadrilateral plate max thickness (mm)			14.77 ± 2.82	0.51	–0.44
Right quadrilateral plate min thickness (mm)			3.46 ± 1.37	0.80	0.11
Left quadrilateral plate min thickness (mm)			3.48 ± 1.32	1.04	0.46
Sex					
Female	48	53.33			
Male	42	46.67			
Screw placement difficulty					
Harder	5	5.56			
Easier	85	94.44			

SD, standard deviation; GSN, greater sciatic notch.

normality based on established guidelines.[20,21] Therefore, parametric statistical tests were used in the comparative analyses (Table I).

Independent samples t-tests were conducted to examine whether screw parameters and QP thickness differed between female and male patients (Table II). Significant sex-based differences were observed across multiple anatomical measurements. Sex-based comparisons are presented in Table II. Men showed significantly longer superior and posterior acetabular screw trajectories bilaterally, whereas acetabular screw angles were significantly smaller in men. Quadrilateral plate thickness (maximum and minimum) was significantly greater in men on both sides, representing the largest effect sizes (d > 1.0). No significant sex differences were observed for GSN screw length or GSN screw angle.

The effect sizes ranged from small to large, with the largest differences observed in QP morphology (d > 1.0). These findings indicate consistent sex-related anatomical variation across acetabular screw trajectories and QP thickness (Table 2).

Pearson correlation analyses were conducted to examine the associations between age and first-measurement morphometric parameters (Table III). Age demonstrated small-to-moderate positive correlations with right superior acetabular screw length (r = 0.291, p = 0.005), left superior acetabular screw length (r = 0.213, p = 0.044), and right acetabular screw angle (r = 0.218, p = 0.039). Accordingly, increasing age was associated with slightly longer superior acetabular screw trajectories and a modest increase in right-sided acetabular screw angulation. Although this pattern could reflect age-related changes in pelvic morphology, such as cortical remodeling, alterations in pelvic tilt, or dimensional widening, which could influence optimal screw path planning, the proportion of explained variance in these models was relatively small ($R^2 \approx 0.05$-0.08), indicating that age alone accounted for only a limited portion of the variability in these morphometric parameters. No significant correlations were observed between age and GSN screw lengths or screw angles (all $p > 0.05$). Similarly, age was not significantly associated with QP maximum or minimum thickness on either side (all $p > 0.05$). Accordingly, the sciatic notch corridor dimensions and QP thickness remained relatively stable across age groups in this sample (Table III). Overall, the correlation pattern showed that although most morphometric parameters were age-independent, age exerted a modest but measurable effect on superior acetabular screw length and right-sided acetabular screw angulation.

As age showed several significant bivariate correlations with acetabular morphometric parameters, three univariate linear regression models were conducted to further quantify age's predictive effect on these outcomes (Table IV). Across all models, age emerged as a statistically significant predictor. Age significantly predicted right superior acetabular screw length (B = 0.113, SE = 0.040, β = 0.291, p = 0.005), left superior acetabular screw length (B = 0.081, SE = 0.040, β = 0.213, p = 0.044), and right acetabular screw angle (B = 0.077, SE = 0.037, β = 0.218, p = 0.039). Although the effect sizes were modest (R^2 = 0.045-0.085), these models showed that older age was associated with slightly longer superior acetabular screw trajectories and marginally greater right-sided acetabular screw angulation. No other morphometric parameters showed significant associations with age in either correlational or regression analyses, suggesting that most acetabular and QP dimensions remained relatively stable across adulthood (Table IV).

Paired samples t-tests were conducted to compare right- and left-sided morphometric measurements. Overall, most right-left comparisons did not yield statistically significant differences. The GSN screw length, superior and posterior acetabular screw lengths, as well as QP maximum and minimum thicknesses, showed no meaningful side-to-side variation (all p > 0.10). The GSN screw angle demonstrated a non-significant trend toward slightly higher values on the right (mean difference = 1.81°, p = 0.078), but this did not reach the threshold for statistical significance. In contrast, the acetabular screw angle showed a significant right-left difference, with right-sided angles modestly but significantly larger than left-sided angles (mean difference = 1.60°, 95% CI [0.54, 2.67], p = 0.004, d = 0.32). Only acetabular screw angle differed significantly between sides, with slightly larger right-sided angles (Table V).

During exploratory analysis, independent samples t-tests were conducted to compare morphometric parameters between cases rated as "harder" (n = 5) versus "easier" (n = 85) screw placement (Table 6). Given the highly unbalanced group sizes, results were interpreted as exploratory. Patients in the "harder" group demonstrated significantly longer GSN screw trajectories on both sides (right: p = 0.021; left: p = 0.006) and significantly thinner QP morphology, with lower maximum thickness bilaterally (right: p = 0.017;

TABLE II
Comparison of the measurement of screw and bone parameters by sex

Variables	Mean ± SD (F)	Mean ± SD (M)	t	*p*	Mean difference	95% CI	Cohen's d
Right GSN screw length (mm)	23.10 ± 4.25	22.77 ± 4.05	0.366	0.714	0.32	–1.42 to 2.07	0.08
Right superior acetabular screw length (mm)	41.83 ± 6.39	44.96 ± 6.75	–2.255	**0.027****	–3.12	–5.88 to –0.37	–0.48
Right posterior acetabular screw length (mm)	71.69 ± 6.54	76.99 ± 7.58	–3.557	**< 0.001***	–5.29	–8.25 to –2.34	–0.75
Left GSN screw length (mm)	23.97 ± 5.11	22.93 ± 3.21	1.129	0.262	1.03	–0.79 to 2.85	0.24
Left superior acetabular screw length (mm)	39.69 ± 5.20	45.38 ± 6.64	–4.553	**< 0.001***	–5.69	–8.17 to –3.21	–0.96
Left posterior acetabular screw length (mm)	70.27 ± 5.26	76.58 ± 7.07	–4.844	**< 0.001***	–6.31	–8.90 to –3.72	–1.02
Right GSN screw angle (°)	112.78 ± 8.39	110.92 ± 8.95	1.021	0.310	1.87	–1.77 to 5.50	0.22
Left GSN screw angle (°)	109.30 ± 9.44	111.03 ± 8.43	–0.911	0.365	–1.73	–5.50 to 2.04	–0.19
Right acetabular screw angle (°)	127.35 ± 5.52	124.16 ± 6.24	2.576	**0.012****	3.19	0.73 to 5.66	0.54
Left acetabular screw angle (°)	125.59 ± 4.43	122.74 ± 5.72	2.668	**0.009****	2.86	0.73 to 4.99	0.56
Right quadrilateral plate max thickness (mm)	13.46 ± 1.99	16.48 ± 2.63	–6.176	**< 0.001***	–3.01	–3.98 to –2.04	–1.31
Left quadrilateral plate max thickness (mm)	13.36 ± 2.01	16.38 ± 2.75	–6.012	**< 0.001***	–3.03	–4.03 to –2.03	–1.27
Right quadrilateral plate min thickness (mm)	3.01 ± 1.18	3.98 ± 1.39	–3.583	**< 0.001***	–0.97	–1.51 to –0.43	–0.76
Left quadrilateral plate min thickness (mm)	2.89 ± 0.82	4.16 ± 1.46	–5.163	**< 0.001***	–1.27	–1.76 to –0.78	–1.09

SD, standard deviation; CI, confidence interval; GSN, greater sciatic notch; t: Independent Samples t-test, * $p < 0.001$, ** $p < 0.05$.

TABLE III

Means, standard deviations, and Pearson correlations for all continuous variables (n = 90)

	Variables	1	2	3	4	5	6	7	8	9	10	11	12	13	14	15
1	Age (year)	-														
2	Right GSN screw length (mm)	0.13	-													
3	Right superior acetabular screw length (mm)	**0.29****	0.13	-												
4	Right posterior acetabular screw length (mm)	0.20	**0.38****	**0.81****	-											
5	Left GSN screw length (mm)	0.05	**0.57****	0.16	0.24*	-										
6	Left superior acetabular screw length (mm)	**0.21***	0.10	**0.64****	**0.57****	0.05	-									
7	Left posterior acetabular screw length (mm)	0.14	0.27**	**0.57****	**0.71****	**0.32****	**0.83****	-								
8	Right GSN screw angle (°)	0.05	0.16	**0.62****	**0.61****	0.14	0.27*	0.29**	-							
9	Left GSN screw angle (°)	−0.09	0.13	0.24*	0.25*	0.04	**0.52****	**0.44****	**0.41****	-						
10	Right acetabular screw angle (°)	**0.22***	**0.38****	**0.49****	**0.48****	0.21	0.06	0.11	**0.57****	0.09	-					
11	Left acetabular screw angle (°)	0.05	**0.30****	0.17	0.17	0.25*	0.26*	0.29**	0.24*	**0.37****	**0.60****	-				
12	Right QP maximum thickness (mm)	−0.13	−0.18	0.23*	**0.35****	−0.05	**0.40****	**0.40****	0.03	0.09	−0.25*	−0.24*	-			
13	Left QP maximum thickness (mm)	−0.09	−0.11	0.18	**0.37****	−0.03	**0.30****	**0.39****	0.06	0.07	−0.16	−0.25*	**0.86****	-		
14	Right QP minimum thickness (mm)	−0.12	−0.19	−0.01	0.04	−0.21*	0.15	0.06	−0.03	0.08	−0.34**	−0.34**	**0.34****	**0.28****	-	
15	Left QP minimum thickness (mm)	−0.15	−0.25*	−0.11	−0.03	−0.25*	0.12	0.08	−0.18	0.06	−0.52**	−0.44**	**0.43****	**0.39****	**0.83****	-

GSN, greater sciatic notch; QP, quadrilateral plate; * $p < 0.05$; ** $p < 0.01$.

TABLE IV
Univariate linear regression analyses examining the association between age and acetabular morphometric parameters

Dependent variable	B	SE(B)	β	t	*p*	R^2	F	Model (*p*)
Right superior acetabular screw length (mm)	0.113	0.040	0.291	2.85	**0.005***	0.085	8.12	0.005
Left superior acetabular screw length (mm)	0.081	0.040	0.213	2.04	**0.044***	0.045	4.17	0.044
Right acetabular screw angle (°)	0.077	0.037	0.218	2.10	**0.039***	0.048	4.41	0.039

B, unstandardized regression coefficient; SE, standard error; β, standardized coefficient; CI, confidence interval. Results from univariate linear regression models assessing the effect of age on morphometric parameters. All three models demonstrated statistically significant associations ($p < 0.05$).

TABLE V
Paired-samples comparisons of right-left morphometric measurements (n = 90)

Pair	Measure	Mean ± SD (Right)	Mean ± SD (Left)	Mean difference	95% CI	t(89)	*p*	Effect size (d)
1	GSN screw length (mm)	22.95 ± 4.14	23.48 ± 4.34	–0.54	–1.36 to 0.28	–1.30	0.196	–0.14
2	Superior acetabular screw length (mm)	43.29 ± 6.71	42.34 ± 6.54	0.95	–0.22 to 2.12	1.61	0.112	0.17
3	Posterior acetabular screw length (mm)	74.16 ± 7.49	73.21 ± 6.90	0.95	–0.21 to 2.11	1.63	0.107	0.17
4	GSN screw angle (°)	111.91 ± 8.66	110.11 ± 8.98	1.81	–0.21 to 3.82	1.78	.078	0.19
5	Acetabular screw angle (°)	125.86 ± 6.05	124.26 ± 5.24	1.60	**0.54 to 2.67**	**2.99**	**0.004***	**0.32**
6	QP max thickness (mm)	14.87 ± 2.75	14.77 ± 2.82	0.10	–0.21 to 0.41	0.63	0.532	0.07
7	QP min thickness (mm)	3.46 ± 1.37	3.48 ± 1.32	0.02	–0.14 to 0.18	0.24	0.810	0.03

SD, standard deviation; QP, quadrilateral plate; * $p < 0.05$.

left: $p = 0.004$). In contrast, the "harder" group showed significantly shorter right-sided superior and posterior acetabular screw lengths ($p = 0.028$ and $p = 0.042$, respectively). Minimum QP thickness showed a similar trend, approaching significance on the right side ($p = 0.052$). No significant between-group differences were observed in GSN or acetabular screw angles (all $p > 0.19$) (Table VI).

The inter-observer reliability was evaluated using a two-way mixed-effects ICC with an absolute-agreement, single-measures definition. Across all morphometric parameters, agreement between observers was consistently high. ICC values for screw lengths, screw angles, and maximum QP thickness ranged from 0.916 to 0.988, indicating excellent reliability. Only the minimum QP thickness demonstrated slightly lower, but still acceptable, agreement (ICC = 0.759-0.784). Intra-observer reliability was evaluated using a two-way mixed-effects model with absolute-agreement criteria. Across all morphometric parameters, including screw lengths, screw angles, and QP thickness, repeat measurements demonstrated excellent reproducibility, with ICC values generally ranging from 0.903 to 0.996. Only the minimum QP thickness displayed slightly lower agreement, with ICC values between 0.820 and 0.845.[22] These findings showed strong measurement stability for repeated assessments conducted by the same observer and supported the precision and consistency of the morphometric evaluation protocol.

DISCUSSION

In the present study, we anatomically defined a GSN–based transcolumnar "magic screw" corridor using 3D CT morphometry. By using the midpoint of the GSN as a reproducible posterior entry landmark and applying standardized Mimics software-aligned views for all measurements, we sought to reduce the variability that limits reproducibility in transcolumnar screw placement described in prior fluoroscopy-dependent techniques.[9] In 90 CT-based reconstructions, the GSN-midpoint trajectory was feasible in the vast majority of cases, providing a consistent transcolumnar corridor and supporting its use for preoperative planning. The posterior acetabular screw, the core of this construct, achieved a mean length of 74.16 ± 7.49 mm on the right and 73.21 ± 6.90 mm on the left, while the maximum QP thickness averaged 14.87 ± 2.75 mm. Together, these

TABLE VI
Comparison of the measurement parameters by screw placement difficulty

Variables	Mean ± SD (H)	Mean ± SD (E) (n = 85)	t	*p*	Mean difference	95% CI	Cohen's (d)
Right GSN screw length (mm)	27.07 ± 5.51	22.70 ± 3.95	2.354	**0.021**	4.37	0.68 to 8.06	1.08
Right superior acetabular screw length (mm)	36.92 ± 3.78	43.66 ± 6.67	–2.233	**0.028**	–6.74	–12.74 to –0.74	–1.03
Right posterior acetabular screw length (mm)	67.56 ± 4.29	74.55 ± 7.47	–2.064	**0.042**	–6.99	–13.72 to –0.26	–0.95
Left GSN screw length (mm)	28.60 ± 8.62	23.18 ± 3.84	2.817	**0.006**	5.42	1.59 to 9.24	1.30
Left superior acetabular screw length (mm)	37.70 ± 5.22	42.61 ± 6.53	–1.650	0.103	–4.92	–10.84 to 1.01	–0.76
Left posterior acetabular screw length (mm)	69.25 ± 6.44	73.45 ± 6.89	–1.328	0.188	–4.20	–10.48 to 2.08	–0.61
Right GSN screw angle (°)	106.96 ± 4.04	112.20 ± 8.78	–1.322	0.190	–5.25	–13.13 to 2.64	–0.61
Left GSN screw angle (°)	110.68 ± 6.85	110.07 ± 9.12	0.146	0.884	0.61	–7.65 to 8.86	0.07
Right acetabular screw angle (°)	125.02 ± 2.34	125.91 ± 6.20	–0.320	0.750	–0.90	–6.46 to 4.67	–0.15
Left acetabular screw angle (°)	126.11 ± 5.89	124.15 ± 5.22	0.812	0.419	1.96	–2.84 to 6.76	0.37
Right quadrilateral plate max thickness (mm)	12.04 ± 0.75	15.03 ± 2.73	–2.433	**0.017**	–3.00	–5.44 to –0.55	–1.12
Left quadrilateral plate max thickness (mm)	11.33 ± 0.53	14.97 ± 2.77	–2.925	**0.004**	–3.64	–6.11 to –1.17	–1.35
Right quadrilateral plate min thickness (mm)	2.31 ± 1.01	3.53 ± 1.36	–1.973	0.052	–1.22	–2.45 to 0.01	–0.91
Left quadrilateral plate min thickness (mm)	2.64 ± 0.33	3.53 ± 1.34	–1.479	0.143	–0.89	–2.10 to 0.31	–0.68

t, Independent samples t-test; F, female; M, male; GSN, greater sciatic notch; * $p < 0.001$; ** $p < 0.05$.

findings provide an anatomy-based framework that complements existing descriptions of the magic screw corridor and offers quantitative parameters for preoperative planning.[4,8,23]

In cases of high-energy acetabular trauma, fixation strategies that stabilize both the posterior and anterior columns during a single operative session are may be valuable, as they can facilitate anatomical reduction of complex patterns without requiring multiple surgical positions or staged procedures. The so-called "magic screw" is so named since, when successfully placed, it provides a transcolumnar construct spanning both columns, capable of supporting posterior column stability while extending toward the anterior column.[12] However, despite growing interest in percutaneous and transcolumnar screw fixation, there is substantial methodological heterogeneity in the literature, ranging from procedural descriptions dependent on fluoroscopy to CT-based anatomical simulations and small clinical series.[4,9,24] This variability indicates that a universally accepted, anatomy-based methodology for corridor definition and reproducible entry landmark selection has yet to be established. Our study differs from previous reports in that we have systematically simulated a GSN-midpoint-based transcolumnar screw corridor on non-pathological pelvic CT reconstructions, combining topographic trajectory characterization with QP thickness assessment as a corridor-limiting factor. These findings suggest that an anatomically standardized guide for a single-position transcolumnar fixation concept may support preoperative planning and help reduce uncertainty during this technically demanding procedure, particularly in fracture patterns requiring simultaneous anterior and posterior column stabilization.

In addition to reproducibility, the GSN midpoint may represent a clinically significant posterior reference point in terms of local neurovascular safety. The GSN region is anatomically related to important neurovascular structures, including the superior gluteal vessels and nerve. These structures exit the pelvis through the superior portion of the notch and may be encountered, particularly during cranially directed posterior dissection or instrumentation.[16] However, standardizing the entry point at the mid-notch region, rather than at a more cranial posterior cortical point, may reduce the likelihood of overlap with the superior gluteal neurovascular bundle. Additionally, strict intraosseous screw advancement with multiplanar verification reduces the risk of extraosseous deviation in the notch region. As sciatic nerve injury is one of the most clinically relevant neurological complications associated with acetabular fractures and their surgical management, defining consistent posterior landmarks and corridor geometry could help to make minimally invasive transcolumnar fixation strategies safer.[18] Nevertheless, careful soft-tissue protection and intraoperative imaging confirmation remain essential when translating an anatomically feasible corridor into clinical practice.

Our morphometric corridor definition aligns with previous virtual and cadaveric simulations. Li et al.[9] reported a mean cylinder length of 73 mm, which is consistent with our average posterior screw length of approximately 74 mm. Furthermore, CT-based work has emphasized the importance of defining entry location and angular orientation to ensure a safe intraosseous passage.[4,9] In this context, our methodology adds value by anchoring the corridor to a consistent posterior landmark (GSN midpoint) and by reporting bilateral corridor characteristics (lengths and angles) obtained under standardized, software-aligned pelvic orientations.[9]

Quadrilateral plate morphology emerged as the most critical anatomical constraint for this trajectory. In the current study, we found a mean minimum QP thickness of 3.46 ± 1.37 mm, whereas the maximum thickness was 14.87 ± 2.75 mm. As our trajectory optimization prioritized an intraosseous path that avoided both cortical breach and intra-articular penetration (as verified in multiplanar views), QP thickness effectively functioned as the limiting "safety margin" along the medial acetabular wall. Percutaneous screw fixation techniques have been increasingly applied in pelvic and periacetabular trauma, highlighting the need for safe and reproducible intraosseous corridors in complex fixation scenarios.[23] Accordingly, our results support the practical implication that safe transcolumnar placement is most reliable when the screw remains within the thicker regions of the corridor, emphasizing the need for patient-specific CT-based simulation in preoperative planning.[8,9] Minor deviations from the planned angulation may reduce the intraosseous margin of safety, reinforcing careful trajectory planning and intraoperative verification consistent with prior technical guidance.[9,25]

In addition to ensuring intra-articular safety, controlling the anterior exit is a clinically relevant aspect of this procedure. Advancing the screw tip into the anterior pubic ramus rather than stopping at the anterior acetabular margin may reduce the risk of anterior cortical breach and potential injury to adjacent neurovascular structures, particularly the external iliac vessels. Anatomical studies have shown that malpositioned acetabular screws (medially or anterosuperiorly) may penetrate or come close to the external iliac vein and other medial pelvic vascular structures.[26,27] Therefore, ensuring that the screw remains fully embedded within the pubic ramus provides an additional safety measure by avoiding sharp anterior prominence and unintended contact with the vessels of the pelvic brim. This anterior column engagement also offers a practical advantage in fracture patterns extending toward the anterior column or pubic root. Here, a single transcolumnar construct could stabilize the posterior column and indirectly support the anterior column via pubic ramus purchase, provided the screw remains intraosseous within the pubic ramus and avoids QP cortical violation.

Sex differences were statistically significant across several primary measurements. Men had significantly longer superior and posterior acetabular screw trajectories, and QP thickness exhibited the most pronounced dimorphism, with men demonstrating notably higher maximum thickness (right: 16.48 ± 2.63 mm *vs.* 13.46 ± 1.99 mm, $p < 0.001$) and higher minimum thickness bilaterally. These findings are clinically relevant, as they indicate that the same nominal corridor may have different tolerances for screw diameter and angulation in female versus male pelves, even when the entry landmark is consistent. Prior CT-based analyses similarly note sex-related differences in pelvic morphology that may narrow the available intraosseous corridor in females.[4] Therefore, when planning a GSN-based transcolumnar screw, sex-related morphological variation, particularly in QP thickness, should be considered to minimize the risk of cortical violation. Consistent with this concept, our data suggest that individualized assessment of corridor dimensions (rather than a uniform implant strategy) may be most appropriate, particularly in patients with thinner QP morphology.

Our exploratory subgroup analysis of the "harder" feasibility group (n = 5) revealed distinct morphological differences. Although this group had longer GSN entry segments (right: 27.07 ± 5.51 mm *vs.* 22.70 ± 3.95 mm), they demonstrated shorter right superior and posterior acetabular screw lengths and significantly thinner maximum QP thickness bilaterally. This pattern suggests that "hard" feasibility may reflect a constrained intraosseous corridor in the periacetabular region rather than inadequate posterior entry length, and that QP thickness may be a key discriminator of corridor permissiveness. However, these findings should be interpreted cautiously given the very small and unbalanced subgroup size. Since multiple morphometric parameters were examined simultaneously, the possibility of type 1 error inflation should be considered when interpreting statistically significant findings. Nevertheless, the direction and magnitude of differences observed in QP thickness in this subgroup are consistent with the broader conclusion that medial wall morphology is the dominant limiting factor for safe placement.[8]

The effects of age and laterality on the corridor appeared to be limited. We found weak positive correlations between age and right superior acetabular screw length and right acetabular screw angle, and regression analysis identified age as a statistically significant predictor of these outcomes; however, the explained variance was low ($R^2 \leq 0.085$), suggesting that individual morphology is more influential than chronological age. More importantly, QP thickness did not correlate significantly with age in our cohort, indicating that the corridor's medial wall thickness may remain relatively stable across adulthood within the sampled population. Prior studies have described age-related changes in cortical thickness distribution along the quadrilateral surface, which may influence fixation strength in older individuals.[8] Therefore, even if corridor geometry remains feasible, bone quality and local cortical distribution should still be considered when extrapolating morphometric feasibility to predict intraoperative screw purchase, particularly in elderly patients.[8] Regarding laterality, the only significant right-left difference was a modestly larger right-sided acetabular screw angle (mean difference = 1.60°, $p = 0.004$), while other parameters showed no meaningful asymmetry, supporting largely bilateral symmetry for preoperative planning.

From a workflow perspective, our methodology was designed to mirror preoperative planning steps that can be replicated in clinical practice: (1) identify the GSN midpoint as a posterior entry landmark, (2) simulate a transcolumnar intraosseous path under standardized pelvic orientations, and (3) verify containment and joint safety using multiplanar reconstructions. This anatomy-driven approach may help reduce dependence on highly specific fluoroscopic positioning and may facilitate more predictable screw placement planning, particularly in fracture patterns involving the QP where medial buttress support is desired.[3,7,9] Nonetheless, intraoperative imaging remains essential, and adherence to established fluoroscopic principles and safety checks is recommended when translating a planned corridor into actual screw placement.[9,14]

The complex, 3D morphology of the pelvis is a well-recognized challenge in acetabular fracture surgery. One of the motivations behind this study was to explore whether the technical difficulties encountered during transcolumnar fixation could be related to individual anatomical variability of pelvic osseous structures. In this context, we attempted to identify a posterior landmark that is both surgically practical and recognizable, and which could provide common guidance despite interindividual morphological differences. Our observations confirmed that, even in anatomically intact pelves, there is considerable difference in QP thickness, acetabular geometry and intraosseous corridor dimensions. These differences may be accentuated further in displaced fractures, where fragment migration and loss of anatomical alignment introduce additional procedural complexity. Therefore, defining an anatomy-based reference framework derived from intact pelvic models could provide a preliminary aid for surgical planning, while acknowledging that fracture-specific reduction patterns and patient-specific morphology are critical factors in determining operative strategy.

Nonetheless, this study has several limitations. As the present analysis was conducted using non-fractured pelvic models, the clinical applicability of the defined transcolumnar corridor in displaced acetabular fractures may be influenced by fracture configuration, medial wall comminution, and intraoperative anatomical distortion. These factors may alter corridor geometry and screw containment safety. Therefore, the current findings should be interpreted primarily as an anatomical feasibility reference framework that requires patient-specific evaluation in fracture settings. From a methodological perspective, first, the retrospective design used non-fractured healthy pelvic models, which does not account for fragment displacement or hematoma formation that can obscure landmarks in clinical trauma. Second, our feasibility assessments were conducted via virtual simulation without biomechanical testing to compare stability against traditional plates. Third, the "harder" feasibility subgroup was very small (n = 5), limiting the statistical power of those exploratory comparisons. Therefore, these analyses should be interpreted cautiously and considered descriptive and hypothesis-generating rather than definitive inferential evidence. In addition, although standardized digital realignment procedures and predefined anatomical reference landmarks were used to improve measurement consistency, the virtual trajectory optimization process inherently involved manual adjustments under multiplanar visualization. Therefore, a certain degree of operator-dependent variability cannot be entirely excluded. However, this potential variability was minimized by applying a stepwise simulation protocol, maintaining predefined cortical safety margins, and confirming reproducibility through inter- and intraobserver reliability analyses. Furthermore, there was a lack of biomechanical validation, such as pull-out strength testing, finite element simulation or cadaveric stability assessment. Although QP morphology appeared to influence corridor feasibility, its direct effect on fixation stability could not be demonstrated within the scope of this anatomical study. As fixation stability is a key factor in the management of acetabular fractures, future studies should incorporate biomechanical modelling, cadaveric testing and clinical validation to better understand the practical importance of the proposed transcolumnar trajectory. Additionally, the present analysis did not incorporate fracture simulation models, assessment of bone mineral quality, or evaluation of potential ethnic anatomical variability. All of these factors may influence corridor morphology and fixation stability in clinical practice. Future studies that integrate fracture-specific modelling, bone quality parameters and multi-population anatomical datasets may provide a more comprehensive understanding of the feasibility and safety of transcolumnar screws.

In conclusion, this 3D CT-based morphometric study describes a GSN–referenced transcolumnar screw pathway that appears anatomically feasible in most adult pelves. The findings demonstrate considerable variability in pelvic osseous morphology, particularly in QP thickness, which may influence intraosseous corridor dimensions and trajectory safety. By integrating a recognizable posterior bony landmark with standardized virtual trajectory simulation and multiplanar verification, the present workflow offers an anatomy-oriented framework that may assist preoperative planning of selected acetabular fixation strategies. Furthermore, careful intraoperative imaging guidance and individualized assessment remain essential when applying such anatomical concepts in clinical fracture settings. We believe that further clinical and biomechanical studies may help to clarify the practical implications of this trajectory in complex acetabular injuries.

Data Sharing Statement: The data that support the findings of this study are available from the corresponding author upon reasonable request.

Author Contributions: P.İ., C.K.: Idea/concept, literature review, references and fundings; C.K.: Design; A.B.: Control/supervision; P.İ., E.U.: Data collection and/or processing; P.İ.: Analysis and/or interpretation, writing the article, other; C.K., A.B.: Critical review; P.İ, A.B.: Materials.

Conflict of Interest: The authors declared no conflicts of interest with respect to the authorship and/or publication of this article.

Funding: The authors received no financial support for the research and/or authorship of this article.

AI Disclosure: The authors declare that artificial intelligence (AI) tools were not used, or were used solely for language editing, and had no role in data analysis, interpretation, or the formulation of conclusions. All scientific content, data interpretation, and conclusions are the sole responsibility of the authors. The authors further confirm that AI tools were not used to generate, fabricate, or 'hallucinate' references, and that all references have been carefully verified for accuracy.

REFERENCES

1. Qi X, Zhang X, Zhang Q, Zhang Y, Huang S, Lv Y, et al. Clinical efficacy and biomechanical analysis of robotic internal fixation with percutaneous screws in the treatment of both-column acetabular fractures. Sci Rep 2025;15:22908. doi: 10.1038/s41598-025-06168-6.
2. Alsheikh KA, Alzahrani AM, Alshehri AS, Alzahrani FA, Alqahtani YS, Alhumaidan MI, et al. Clinical outcomes of percutaneous screw fixation of acetabular fracture: A minimally invasive procedure. J Taibah Univ Med Sci 2022;18:279-86. doi: 10.1016/j.jtumed.2022.09.015.
3. Gänsslen A, Lindahl J, Lindtner RA, Krappinger D, Staresinic M. Special screw corridors and imaging in pelvic

ring trauma. Arch Orthop Trauma Surg 2025;145:110. doi: 10.1007/s00402-024-05610-0.

4. Lu H, Gong X, Xuan C, Lu Q. CT Imaging anatomical study of percutaneous magic screw fixation for acetabular posterior column fracture. Research Square [Preprint] 2022. doi: 10.21203/rs.3.rs-1271947/v1.
5. Serra M, Solano A, Godinho M, Mereddy P, Baron ML, Mauffrey C. Acetabular reconstruction: from fracture pattern to fixation-part 2. Injury 2025;56:112781. doi: 10.1016/j.injury.2025.112781.
6. Solano A, Serra M, Mereddy P, Godinho M, Le Baron M, Mauffrey C. Acetabular reconstruction: From fracture pattern to fixation - part 1. Injury 2025;56:112578. doi: 10.1016/j.injury.2025.112578.
7. Freude T, Gänsslen A, Krappinger D, Lindahl J. Quadrilateral plate fractures. Arch Orthop Trauma Surg 2024;145:51. doi: 10.1007/s00402-024-05698-4.
8. Guo J, Dong W, Zhou Y, Hu J, Ye P, Chen W, et al. Differences in fixation to young and elderly quadrilateral surfaces with Anatomic Quadrilateral Surface Plate (AQSP) based on cortical thickness morphological results. J Orthop Surg Res 2022;17:143. doi: 10.1186/s13018-022-03027-2.
9. Li J, Li Z, Wang X, Zhang G, Peng Y, Zhang S, et al. Establishment of fluoroscopy views and standardized procedure of percutaneous magic screw insertion for acetabulum fractures. BMC Musculoskelet Disord 2018;19:332. doi: 10.1186/s12891-018-2228-y.
10. Gupta A, Bansal P, Kumar V, Aggarwal S. Quadrilatral plate stabilization: Conventional reconstruction plate or anatomical plate: A systematic review and meta-analysis. J Clin Orthop Trauma 2025;69:103120. doi: 10.1016/j.jcot.2025.103120.
11. Egli RJ, Keel MJB, Cullmann JL, Bastian JD. Secure screw placement in management of acetabular fractures using the suprapectineal quadrilateral buttress plate. Biomed Res Int 2017;2017:8231301. doi: 10.1155/2017/8231301.
12. Sun Y, Chen J, Li X, Lv F. Safe passage analysis for both column screw fixation technique in posterior column acetabular fractures. Sci Rep 2025;15:44932. doi: 10.1038/s41598-025-29543-9.
13. Zheng L, Hao J, Hu CJ, Shen X, Yang G, Zeng G, et al. Antegrade insertion of full-length ramus screws for the treatment of pelvic and/or acetabular fracture. Injury 2025;56:112669. doi: 10.1016/j.injury.2025.112669.
14. Öztürk V, Bilgili MG. Fluoroscopy-assisted identification of the individual optimal antegrade entry point of the anterior column fixation corridor in pelvic and acetabular surgery: A novel perspective. J Orthop Surg Res 2025;20:635. doi: 10.1186/s13018-025-06027-0.
15. Chanbour H, Roth SG, Chen JW, Uppuganti S, Nyman JS, Ali MA, et al. Do iliac screws placed close to the sciatic notch have greater pullout strength? Oper Neurosurg 2024;27:549-56. doi: 10.1227/ons.0000000000001159.
16. Collinge CA, Ziran NM, Coons DA. Relationship between the superior gluteal vessels and nerve at the greater sciatic notch. Orthopedics 2015;38:e929-33. doi: 10.3928/01477447-20151002-62.
17. van der Merwe JF, Erasmus LJ, van der Merwe W, Ellis JA. Obtaining optimum screw placement for revision acetabular prostheses using the sciatic notch as reference. Transl Res Anat 2021;24:100133. doi: 10.1016/j.tria.2021.100133.
18. Issack PS, Helfet DL. Sciatic nerve injury associated with acetabular fractures. HSS J 2009;5:12-8. doi: 10.1007/s11420-008-9099-y.
19. Field AP. Discovering Statistics Using IBM SPSS Statistics. 6th ed. London: SAGE Publications Ltd; 2024.
20. George D, Mallery P. IBM SPSS Statistics 29 Step by Step: A Simple Guide and Reference. 18th ed. New York: Routledge; 2024.
21. Tabachnick BG, Fidell LS, Ullman JB. Using multivariate statistics. Vol 5. pearson Boston, MA; 2007.
22. Musikachart P, Ariyawatkul T, Wongcharoenwatana J, Piamthipmanas T, Chanchoo S, Eamsobhana P. Intra-observer and inter-observer reliability of shaft condylar angle and lateral capitellohumeral angle: Evaluation based on reliability in different ages and levels of experience. Orthop Surg 2019;11:467-73. doi: 10.1111/os.12489.
23. Starr AJ, Walter JC, Harris RW, Reinert CM, Jones AL. Percutaneous screw fixation of fractures of the iliac wing and fracture-dislocations of the sacro-iliac joint (OTA Types 61-B2.2 and 61-B2.3, or Young-Burgess "lateral compression type II" pelvic fractures). J Orthop Trauma 2002;16:116-23. doi: 10.1097/00005131-200202000-00008.
24. Caviglia H, Mejail A, Landro ME, Vatani N. Percutaneous fixation of acetabular fractures. EFORT Open Rev 2018;3:326-34. doi: 10.1302/2058-5241.3.170054.
25. Öztürk V, Kaya B, Çelik T, Çelik M, Kural C, Bilgili MG. Is the innovative both column screw fixation technique a biomechanical game-changer in the fixation of acetabular posterior column fractures? Int Orthop 2025;49:2271-80. doi: 10.1007/s00264-025-06604-2.
26. Keating EM, Ritter MA, Faris PM. Structures at risk from medially placed acetabular screws. J Bone Joint Surg Am 1990;72:509-11.
27. Shon WY, Gupta NR, Deshmukh SN, Garud AB, Theeppainthan P, Lee KS. Prevention of pernicious vascular event: Acetabular component screw impinging on external iliac vessels - a unique case report. J Orthop Case Rep 2023;13:121-6. doi: 10.13107/jocr.2023.v13.i10.3960.